

ON THE REALIZATION OF DO-OTA-C OSCILLATORS

Hakan Kuntman

Aydın Özpınar

Istanbul Technical University, Faculty of Electrical and Electronics Eng.

Department of Electronics and Communication Engineering

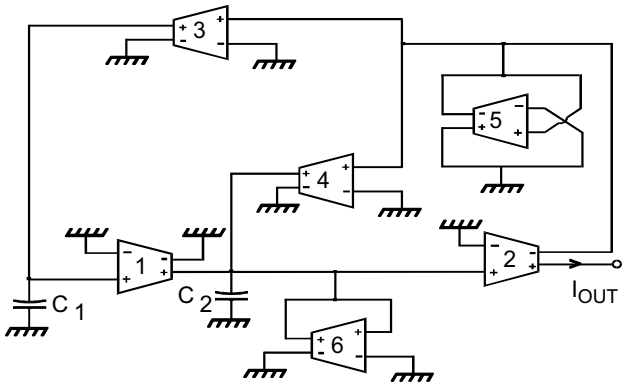
80626, Maslak, Istanbul, TURKEY

Abstract

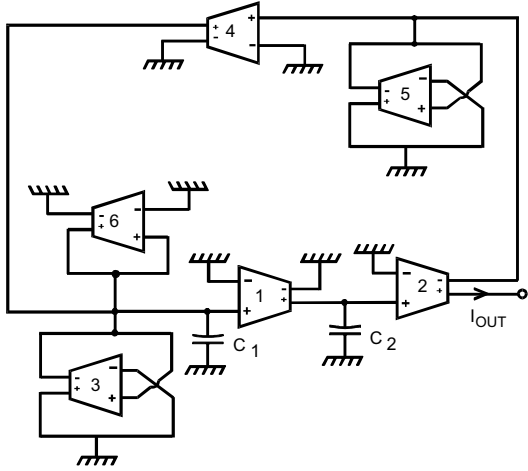
The basic aim of this paper is to give design considerations of current-mode high frequency DO - OTA - C oscillator topologies achieving noninteractive control of b and Ω_0 with a minimum number of components. Starting from DO-OTA-C (grounded capacitor) filter topologies, reported in the literature and employing a minimum number of components, novel DO - OTA - C oscillator topologies are generated by converting of filters into oscillators. Furthermore, the influence of the OTA nonidealities on oscillator performance is investigated by including the finite input and output impedances and transconductance frequency dependencies of DO-OTAs into derived equations. The performance of the proposed topologies are demonstrated with SPICE simulation program

Reference

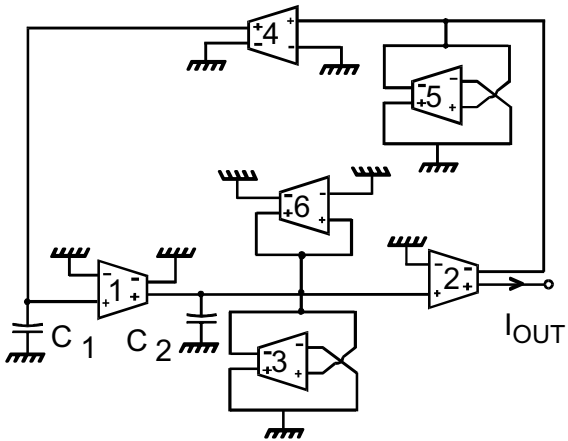
H. Kuntman, A. Özpınar, On the realization of DO-OTA-C oscillators, Microelectronics Journal, Vol.29, No. 12, pp.991-997, 1998.



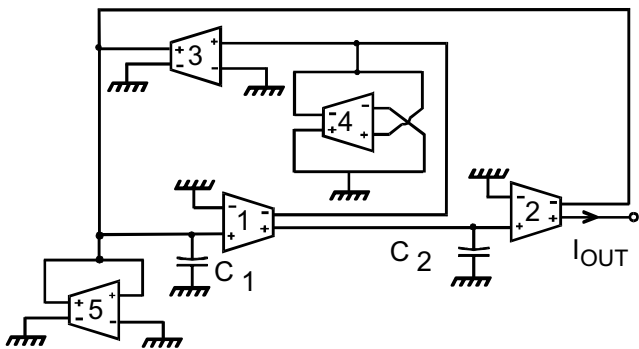
(a)



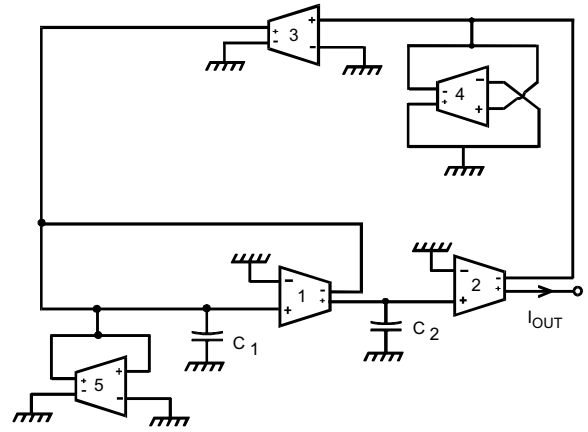
(b)



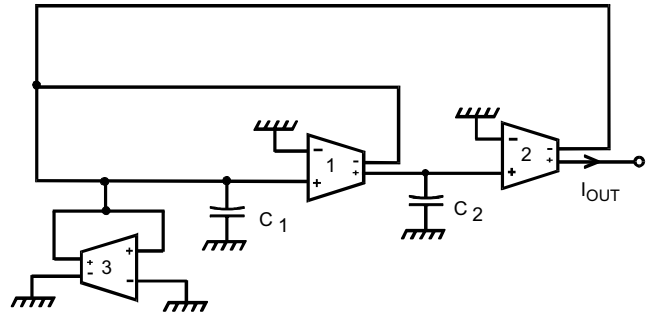
(c)



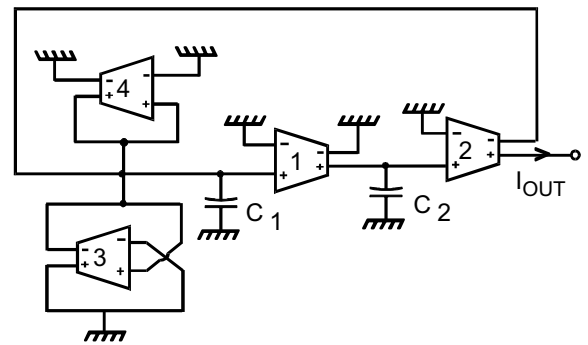
(d)



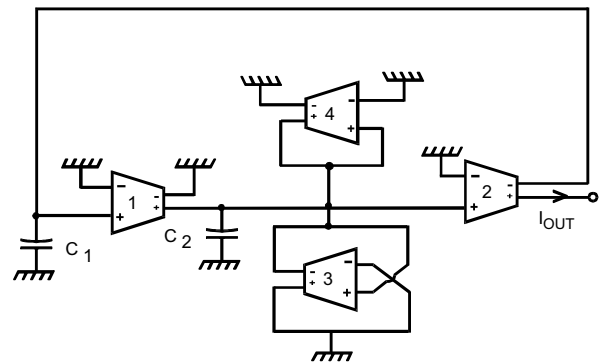
(e)



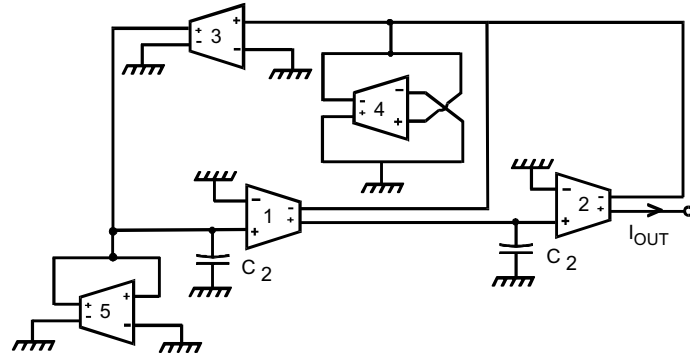
(f)



(g)



(h)



(i)

Figure 1. Proposed DO-OTA-C oscillator topologies.

Table-1. Expressions for oscillation conditions and oscillator frequencies of topologies illustrated in Fig.1, derived assuming ideal OTAs..

| Topology | b | Ω_0^2 |
|-----------|---|---|
| Figure 1a | $\frac{g_{m2} \cdot g_{m4} - g_{m6}}{g_{m5} C_2}$ | $\frac{g_{m1} \cdot g_{m2} \cdot g_{m3}}{C_1 C_2 g_{m5}}$ |
| Figure 1b | $\frac{g_{m3} - g_{m6}}{C_1}$ | $\frac{g_{m1} \cdot g_{m2} \cdot g_{m4}}{C_1 C_2 g_{m5}}$ |
| Figure 1c | $\frac{g_{m3} - g_{m6}}{C_2}$ | $\frac{g_{m1} \cdot g_{m2} \cdot g_{m4}}{C_1 C_2 g_{m5}}$ |
| Figure 1d | $\frac{g_{m1} \cdot g_{m3} - g_{m5}}{g_{m4} C_1}$ | $\frac{g_{m1} \cdot g_{m2}}{C_1 C_2}$ |
| Figure 1e | $\frac{g_{m1} - g_{m5}}{C_1}$ | $\frac{g_{m1} \cdot g_{m2} \cdot g_{m3}}{C_1 C_2 g_{m4}}$ |
| Figure 1f | $\frac{g_{m1} - g_{m3}}{C_1}$ | $\frac{g_{m1} \cdot g_{m2}}{C_1 C_2}$ |
| Figure 1g | $\frac{g_{m3} - g_{m4}}{C_1}$ | $\frac{g_{m1} \cdot g_{m2}}{C_1 C_2}$ |
| Figure 1h | $\frac{g_{m3} - g_{m4}}{C_2}$ | $\frac{g_{m1} \cdot g_{m2}}{C_1 C_2}$ |
| Figure 1i | $\frac{g_{m1} \cdot g_{m3} - g_{m5}}{g_{m4} C_1}$ | $\frac{g_{m1} \cdot g_{m2} \cdot g_{m3}}{C_1 C_2 g_{m4}}$ |

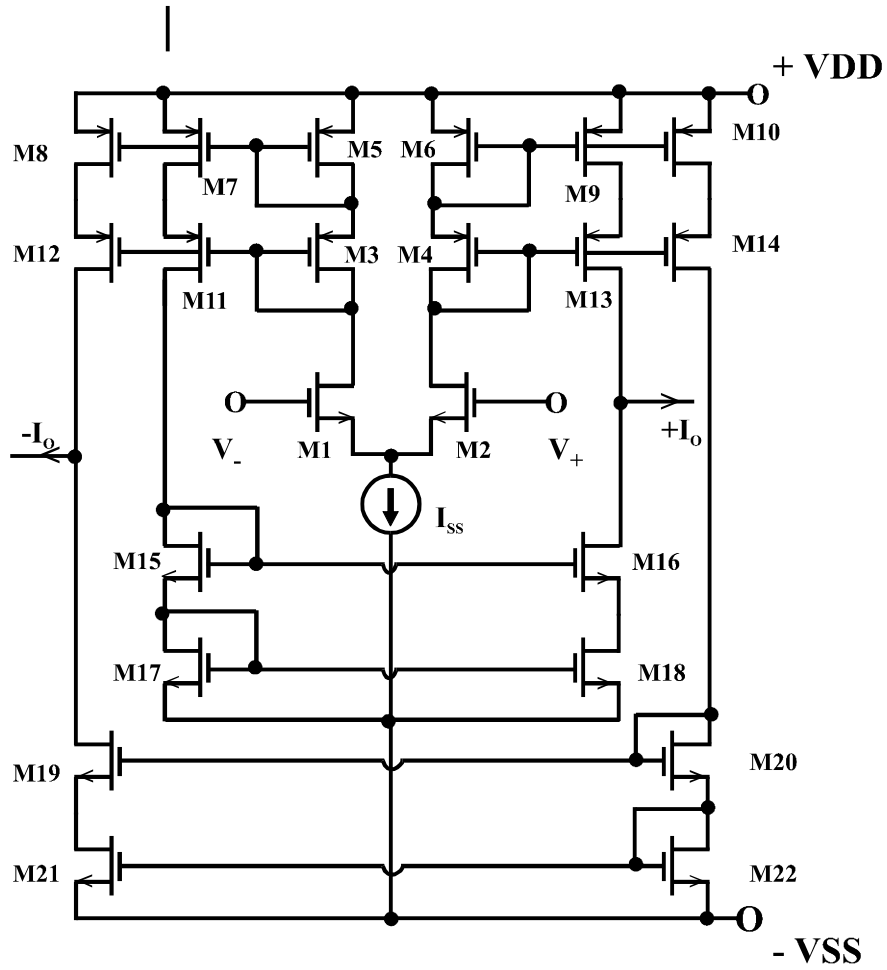


Figure 3. CMOS cascode DO-OTA structure used for SPICE simulations.

Table-3 . Dimensions of MOS transistors in CMOS DO-OTA structure shown in Fig.

| | $W(\mu m)$ | $L(\mu m)$ | | $W(\mu m)$ | $L(\mu m)$ |
|-----|------------|------------|-----|------------|------------|
| M1 | 30 | 3 | M12 | 12 | 3 |
| M2 | 30 | 3 | M13 | 12 | 3 |
| M3 | 12 | 3 | M14 | 12 | 3 |
| M4 | 12 | 3 | M15 | 5 | 3 |
| M5 | 12 | 3 | M16 | 5 | 3 |
| M6 | 12 | 3 | M17 | 5 | 3 |
| M7 | 12 | 3 | M18 | 5 | 3 |
| M8 | 12 | 3 | M19 | 5 | 3 |
| M9 | 12 | 3 | M20 | 5 | 3 |
| M10 | 12 | 3 | M21 | 5 | 3 |
| M11 | 12 | 3 | M22 | 5 | 3 |

Table 6. SPICE simulation results of output current and output voltage performed for different load resistance values.

| Figure 1a | I_{OUTpp} | V_{OUTpp} | frequency |
|--------------------|--------------------------|--------------------------|------------------|
| $R_L = 1 \Omega$ | 376.255 μ A | 376.255 μ V | 1.297MHz |
| $R_L = 1 k\Omega$ | 372.208 μ A | 372.208 mV | |
| $R_L = 10 k\Omega$ | 398.098 μ A | 3.98098 V | |
| Figure 1b | | | |
| $R_L = 1 \Omega$ | 616.392 μ A | 616.392 μ V | 1.357791 MHz |
| $R_L = 1 k\Omega$ | 709.969 μ A | 709.968 mV | |
| $R_L = 10 k\Omega$ | 668.157 μ A | 6.6815 V | |
| Figure 1c | | | |
| $R_L = 1 \Omega$ | 656.413 μ A | 656.413 μ V | 1.4315818 MHz |
| $R_L = 1 k\Omega$ | 649.716 μ A | 649.716mV | |
| $R_L = 10 k\Omega$ | 602.833 μ A | 6.0283 V | |
| Figure 1d | | | |
| $R_L = 1 \Omega$ | 1006.509 μ A | 1006.509 μ V | 1.369527 MHz |
| $R_L = 1 k\Omega$ | 1007.313 μ A | 1007.313 mV | |
| $R_L = 5 k\Omega$ | 975.762 μ A | 4.8788 V | |
| Figure 1e | | | |
| $R_L = 1 \Omega$ | 718.012 μ A | 718.012 uV | 1.3553606 MHz |
| $R_L = 1 k\Omega$ | 720.880 μ A | 720.880 mV | |
| $R_L = 10 k\Omega$ | 688.346 μ A | 6.8835 V | |
| Figure 1f | | | |
| $R_L = 1 \Omega$ | 731.044 μ A | 731.451 uV | 1.365707 MHz |
| $R_L = 1 k\Omega$ | 774.261 μ A | 774.261 mV | |
| $R_L = 10 k\Omega$ | 747.489 μ A | 7.4761 V | |
| Figure 1g | | | |
| $R_L = 1 \Omega$ | 714.922 μ A | 714.922 μ V | 1.3608219 MHz |
| $R_L = 1 k\Omega$ | 736.624 μ A | 736.624 mV | |
| $R_L = 10 k\Omega$ | 699.877 μ A | 6.796 V | |
| Figure 1h | | | |
| $R_L = 1 \Omega$ | 679.074 μ A | 679.074 μ V | 1.349757 MHz |
| $R_L = 1 k\Omega$ | 704.037 μ A | 704.037 mV | |
| $R_L = 10 k\Omega$ | 675.921 μ A | 6.7592 V | |
| Figure 1i | | | |
| $R_L = 1 \Omega$ | 642.317 μ A | 642.317 μ V | 1.509787 MHz |
| $R_L = 1 k\Omega$ | 650.343 μ A | 650.343 mV | |
| $R_L = 10 k\Omega$ | 576.071 μ A | 5.7607 V | |

Table 5. Theoretical and simulation results of oscillation frequency obtained for proposed oscillator topologies

| Topology | Theory | Simulation with actual CMOS DO-OTAs |
|-----------|-----------|-------------------------------------|
| Figure 1a | 1.342 MHz | 1.297 MHz |
| Figure 1b | 1.433 MHz | 1.358 MHz |
| Figure 1c | 1.488 Mhz | 1.431 MHz |
| Figure 1d | 1.472 MHz | 1.37 MHz |
| Figure 1e | 1.433 MHz | 1.355 MHz |
| Figure 1f | 1.433 MHz | 1.365 MHz |
| Figure 1g | 1.433 MHz | 1.36 MHz |
| Figure 1h | 1.433 MHz | 1.35 MHz |
| Figure 1i | 1.537 MHz | 1.509 MHz |

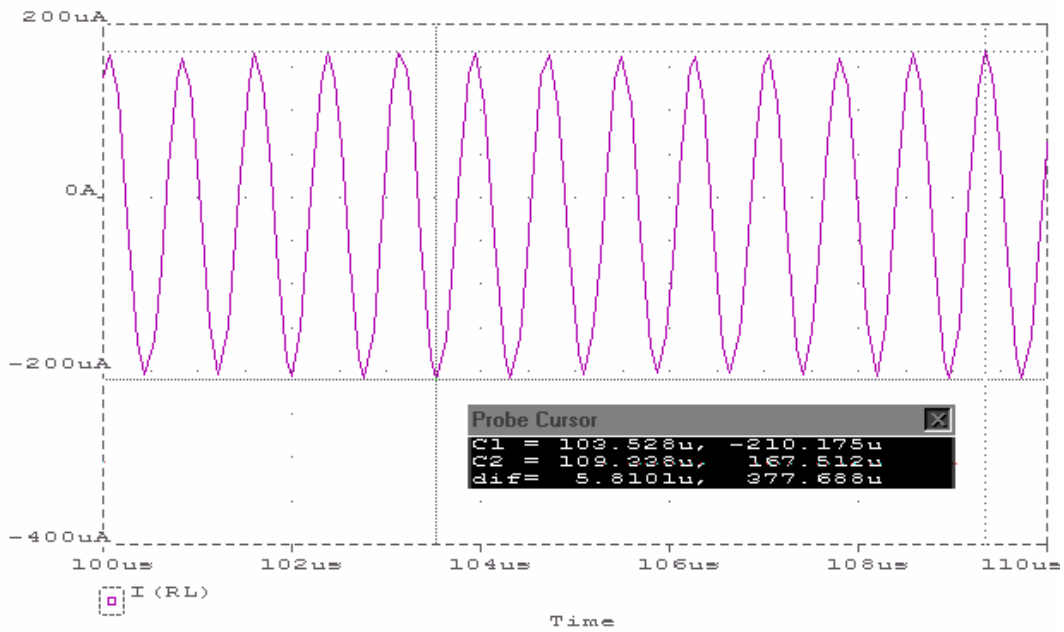


Fig.5. Simulated waveform for output current of oscillator topology illustrated in Fig.1a., $C_1 = C_2 = 50 \text{ pF}$, $RL = 1000 \text{ } \Omega$